

Detection and tracking of MAVs using a LiDAR with rosette scanning pattern

Sándor Gazdag^{1,2}, Tom Möller^{1,3}, Tamás Filep^{1,4}, Anita Keszler¹ and András L. Majdik^{1,2}

Abstract—The usage of commercial Micro Aerial Vehicles (MAVs) has increased drastically during the last decade. While the added value of MAVs to society is apparent, their growing use is also coming with increasing risks like violating public airspace at airports or committing privacy violations. To mitigate these issues it is becoming critical to develop solutions that incorporate the detection and tracking of MAVs with autonomous systems. This work presents a method for the detection and tracking of MAVs using a novel, low-cost rosette scanning LiDAR on a pan-tilt turret. Once the static background is captured, a particle filter is utilized to detect a possible target and track its position with a physical, programmable pan-tilt system. The tracking makes it possible to keep the MAV in the center, maximizing the density of 3D points measured on the target by the LiDAR sensor. The developed algorithm was evaluated within the indoor Micro aerial vehicle and MOTion capture (MIMO) arena and has state-of-the-art tracking accuracy, stability, and fast re-detection time in case of tracking loss. Based on the outdoor tests, it was possible to significantly increase the detection distance and number of returned points compared to other similar methods using LiDAR.

I. INTRODUCTION

Nowadays, the number of drones for different applications is growing rapidly, since they have become affordable and easy to use [1]. Drones have contributed to the development of many fields, such as precision agriculture [2] and modern production [3]. There are many examples in other important areas, e.g. transport industry [4], mining industry [5], and the military domain [6].

In addition to the above, the utilization of drones for hobby purposes is also developing explosively, increasing the risk of inappropriate use. Hobby drones can be used for unauthorized recording, thereby violating people's right

* This work was supported in part by AFOSR Award No. FA8655-23-1-7071, by the European Union within the framework of the National Laboratory for Autonomous Systems (RRF-2.3.1-21-2022-00002), by the Hungarian Scientific Research Fund (No. NKFIH OTKA K-139485), by TKP2021-NVA-01 project and by the Doctoral Excellence Fellowship Programme (DCEP) of the NRD fund and BME under a grant agreement with the NRD office.

¹Sándor Gazdag, Tom Möller, Tamás Filep, Anita Keszler and András L. Majdik are with HUN-REN SZTAKI Institute for Computer Science and Control, Kende u. 13-17, 1111 Budapest, Hungary {sander.gazdag, tom.moller, tamas.filep, keszler.anita, andras.majdik}@sztaki.hun-ren.hu

²Sándor Gazdag and András L. Majdik are also with the Budapest University of Technology and Economics, Kálmán Kandó Doctoral School of Transportation and Vehicle Engineering, Műegyetem rkp. 3. 1111 Budapest, Hungary

³Tom Möller is also with the KTH Royal Institute of Technology and Eötvös Loránd University (ELTE)

⁴Tamás Filep is also with the Eötvös Loránd University, Doctoral School of Informatics, Pázmány P. sétány 1/C, 1117 Budapest, Hungary

to undisturbed privacy [7], [8]. Furthermore, they can also pose a threat to protected buildings (e.g. airports, factories, power plants) [9]. Due to the increased security risks, the development of autonomous drone detection and tracking systems has become a priority area of research.

Several sensors can be used for drone detection, such as radar [10], [11], LiDAR [12], [13], camera [14], [15], [16], radio-frequency [17], [18] and acoustic sensors [19], [20]. The detection efficiency can be further improved by using the sensor fusion method [21], [22]. However, each sensor modality should also give good results when used independently [23].

In this study, we tackle the problem of LiDAR-based detection of drones. The advantage of the LiDAR sensor is that it provides accurate 3D measurement of the environment and the detected objects, in contrast with the other sensors mentioned above.

Novel rosette scanning LiDARs open up new possibilities for the detection of small objects. The rosette scanning Livox LiDAR sensor uses multiple, aligned laser beams, which move in a non-repetitive rosette-like pattern inside the sensor, covering the entire Field of View (FoV) by using a Risley prism. This type of sensor design results in faster measurements, and cheaper devices with fewer moving components compared to the more common rotating models (e.g., Velodyne VLP-16¹, Hesai XT32², Ouster OS2³).

An important feature of the rosette scanning LiDAR is that it captures significantly more measurement data from a target object in the center of the sensor's FoV, as the laser beam passes through the center each time it travels along the rotating 8-like pattern. Towards the outer edges of the FoV, the point cloud becomes sparser, but since it is a non-repetitive scanning technique, the density will still increase over time. These properties allow for new methods in MAV detection and tracking.

This paper advances the state-of-the-art with a new method for drone detection and tracking based on a rosette scanning LiDAR. As the first step of the method, a background model is built to separate the static part of the scene from the moving objects. Next, after preprocessing the incoming point clouds, the position of the drone is computed using a particle filter approach. The pan-tilt turret, controlled based on the drone's estimated position, keeps the drone in the center of the FoV, thereby maximizing the density of 3D points measured on the target by the LiDAR sensor.

¹<https://velodynelidar.com/products/puck/>

²<https://www.hesaitech.com/product/xt32/>

³<https://ouster.com/products/hardware/os2-lidar-sensor>

The proposed method has been validated by performing indoor and outdoor test measurements. The indoor tests were evaluated in the MICRO aerial vehicle and MOTION capture (MIMO) arena [24], [25] and have shown promising results in tracking accuracy, tracking stability, and robust re-detection. We achieved similar accuracy to the state-of-the-art indoor method using a similar sensor [26] while also presenting robust re-detection capabilities. A set of outdoor experiments in various weather conditions were also performed. The outcome of these experiments has shown to increase drone detection efficiency compared to the current state-of-the-art method that uses a circular LiDAR [13]. Namely, our method increases the maximum detection distance by approximately 80 percent with respect to the baseline method in case no special retroreflector marker is applied to the target object. In addition, the number of points reflected from the drone at the same distance increased several times over the full range. A video of the outdoor experiments with the proposed system is available⁴.

The remainder of the paper is organized as follows: related work is presented in section II, the proposed algorithm in section III, the experiments in sections IV and V, and finally the conclusion in section VI.

II. RELATED WORK

Vision-based methods dominate the field of tracking small objects (e.g. [14], [15], [16], [25]). Often these solutions utilize neural networks, such as YOLO [27] to detect and classify objects in images or videos. In contrast, this paper tackles the challenges of drone detection using a LiDAR sensor which provides accurate 3D measurements of the environment and the detected objects. Therefore in this section, LiDAR-based object detection and tracking methods are overviewed with a special focus on small-sized drones.

When looking at LiDAR-based solutions, the algorithms can be categorized into model-based and model-free methods. Model-based tracking algorithms utilize a detection method to distinguish the targets from other objects, using a model of the target. Model-free tracking algorithms compare consecutive scans of the environment to distinguish dynamic objects. Most model-based solutions rely on the shape of the target object or a fixed movement pattern, which does not apply to small and sparse point clouds of MAVs. Model-free approaches, however, are more suitable for a general application, but either rely on bigger objects or on commonly used ring scanning patterns.

Examples for model-based approaches are [28] and [29]. In [28] classifiers are trained with geometrical and statistical features of groups of neighboring points at the same height. The distinguishment of different heights is facilitated by a 360° ring scanning LiDAR. In [29] authors combine a volumetric occupancy map with a 3D convolutional neural network (CNN) applied on LiDAR point clouds. Other neural network approaches include VoxelNet [30], PointNet [31],

and PointNet++ [32]. VoxelNet divides a point cloud into equally spaced 3D voxels and transforms a group of points within each voxel into a unified feature representation. It is applied to LiDAR street scans for detecting objects like pedestrians or cars. PointNet on the other hand directly processes point clouds. It provides an architecture for applications such as object classification and segmentation.

As explained above, model-free solutions are independent of the target object's shape and, therefore more suitable for a wider range of applications with sparse point clouds. In [33] authors present such an approach for detecting and tracking dynamic objects in 3D LiDAR scans that use multiple estimated motion models obtained from within a scene. The motion models are derived from finding point correspondences between two scans. In [34] another model-free method is discussed, where the input is a sequence of dense 3D measurements returned by e.g. multi-layer laser scanners. The next states of an object hypothesis are predicted by a Kalman filter and aligned with the help of an iterative closed point (ICP) algorithm.

In contrast to the just described solutions, which were designed to track objects the size of humans or cars, in the current paper the point cloud resulting from the MAV is containing only a few points. When narrowing the subject down to the detection and tracking of small objects from LiDAR scans the literature is however limited.

The authors of [35] propose a method for detecting and tracking small objects within sparse point clouds generated by a 360° spinning LiDAR with 16 scan rings. The point clouds are segmented based on their width and clustered using the region growth algorithm. Objects are filtered out using geometric features (height range and maximum diagonal width). The hypothesis set contains an axis-aligned bounding box, 3D position, and velocity on which a Kalman filter is applied assuming constant velocity.

The vast majority of the segmentation and detection algorithms are based on having scan rings available [36]. Our work investigates the potential of a rosette scanning LiDAR, which makes methods like the one used in [35] unsuitable.

In [37] a method is proposed for tracking MAVs in a point cloud generated by a static rosette scanning LiDAR, that is further improved in [26]. In these papers, the integration time of the LiDAR frame is dynamically set to adapt to the speed and distance of the target's movement to track MAVs indoors at distances of up to about 30 *m* without the ability to regain tracking if lost. Conversely, our aim is to align the rosette scanning LiDAR to ensure continuous centering of the target drone within the sensor, thereby maximizing the number of returned points. Additionally, our approach incorporates a robust tracking method capable of regaining tracking.

VLP-16 and HDL-64 LiDAR sensors are popular in many related research. In the case of a fixed LiDAR configuration, the usability range in [12] is less than 10 *m* for the VLP16 sensor and 35–50 *m* for the HDL-64 sensor. [13] showed that few hits are sufficient to track the targets. The maximum detecting distance was significantly increased with the method they proposed. Their maximum distance

⁴Video of outside experiments at <https://youtu.be/VdePm3on8vo>

is 70 m , even with a sparse point cloud. By applying retroreflectors this value increased to 100 m . The applied retroreflectors did not increase the size of the drone but increased the number of reflected points by the drone. Our method greatly outperforms this baseline solution in similar weather conditions with a maximum tracking distance of more than 120 m without retroreflectors.

In the case of outdoor measurements, LiDAR sensor performance significantly depends on the weather conditions [38], [39]. According to [40] the detection range of LiDAR sensors break down below 40 m meteorological visibility and is limited to 25 m in such foggy weather conditions. [41] showed smaller changes in the detection distance, while the number of detected points decreased dramatically in rainy weather. Based on these findings a significant reduction in the detection distance and the number of detected points can be expected for outdoor tests under foggy weather conditions. Although this was confirmed by our experiments, our method could still track the drone to a little more than 50 m .

III. THE PROPOSED ALGORITHM

The proposed algorithm is built around a particle filter [42]. The flowchart of our method is presented in Fig. 1, where the main steps of the algorithm are shown. Note on the figure, when the system is installed at a new location, the first step is to build a background model (see Section III-A). This is used to filter the static background from the point cloud to detect the target object.

Next, as part of the object tracking the particle filter performs the prediction step. If there is a new incoming measurement point cloud, the background model is subtracted to reduce static noise (details are given in Section III-B). The three steps of the particle filter (predict, update, and resample) are explained in detail in Section III-C.

Once detected, the drone is kept in the center of the LiDAR's FoV by orienting the pan-tilt turret towards the position computed by the particle filter (see Section III-D). As a result, the measured point density reflected from the drone is maximized.

A. Building the Background Model

The background model is built once at the beginning of the algorithm, hence the background can be considered constant during drone tracking. The turret is set to scanning mode and performs movements to scan a pre-defined area. Because of the LiDAR's non-repetitive way of scanning, the point density of the whole scene will increase the longer the time time for scanning is. After building the background model, the turret switches to tracking mode and is moved by control instructions calculated based on the estimated drone position.

The background model is represented with OctoMap[43]. An OctoMap is an efficient probabilistic 3D mapping framework using octrees. The octree tree structure results in fast access times when querying individual voxels.

Based on the position and orientation of the LiDAR, the incoming point cloud is transformed into the static coordinate system of the background model. The points are filtered

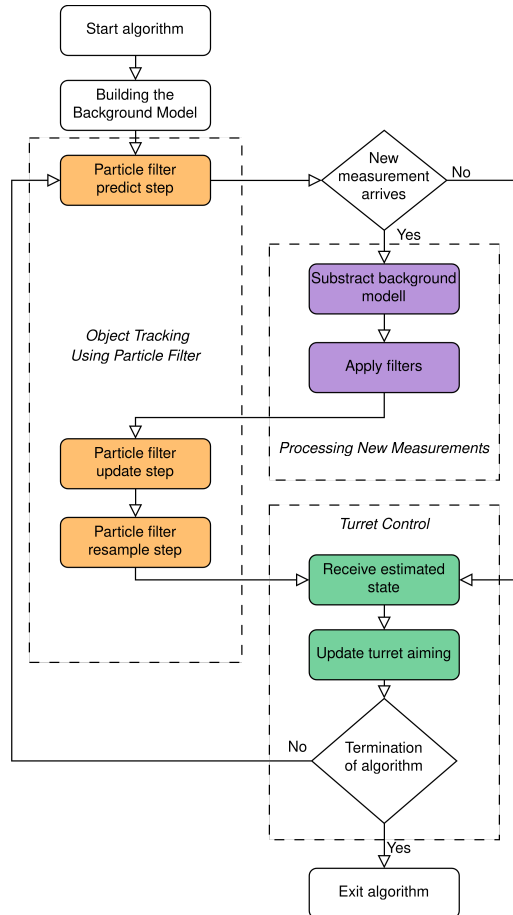


Fig. 1: Overview of the proposed method.

based on position thresholds; the ground plane, near points, and far away points are removed. After filtering, the point cloud is inserted into the OctoMap of the background model. As the last step of building the background model, after inserting all the collected point clouds, inflation is performed to account for measurement noise (e.g. vibrations of the turret base) as well as small changes in background objects (such as leaves moving on the trees).

B. Processing New Measurements

As the first step of processing, distance filters are performed on the incoming data points to remove the ground plane, near points, and far away points than the background model is subtracted. There are two additional filters to remove the reflected points that are not close enough to each other and cannot belong to the target object. The filters are the *RadiusOutlierRemoval* and *StatisticalOutlierRemoval* algorithms from the Point Cloud Library (PCL) [44].

C. Object Tracking Using Particle Filter

The estimated position of the drone is calculated using the particle filter. The particle filter is a recursive, Bayesian state estimator that uses discrete particles to approximate the posterior distribution of an estimated state. Bayes's theorem

is used to refine the belief based on a prior estimate and newly received measurements.

The particle filter's main strength is that it can use both linear and non-linear process and measurement models, unlike other state estimation algorithms e.g. the Kalman filter. Due to the nature of the particle filter, the potential estimated states can also be represented with arbitrarily shaped probability distributions. These properties are welcome since MAVs can have a very wide range of possible movement patterns, with potentially abrupt changes in movement directions and speed in all three dimensions. Furthermore, it is straightforward to update the state of the particles using the LiDAR measurements.

The implementation of the particle filter has three main steps: predict, update, and resample. The prediction step uses the latest state to predict the next state based on the state transition model. The update step uses the incoming filtered point cloud data to refine the state estimate using Bayes' theorem. Finally, the last step is to resample the particles in the state space to match the posterior distribution of the estimated state, thereby solving the degeneracy problem. The particle update and resampling steps are implemented as described in [45] where each particle represents a possible drone position.

D. Turret control

Turret control is possible in two ways: in initialization or tracking mode. During initialization mode, the pan-tilt turret collects data points for a specified time in a predefined area to build the background model. In tracking mode, the control commands are calculated based on the current position of the turret and the estimated position of the drone. The tracking mode aims to keep the drone in the middle of the FoV to maximize the density of reflected points from the drone.

E. Implementation details

The Robot Operating System (ROS) was used to integrate and communicate with the program components. ROS provides a very capable framework to create modular program nodes and let them communicate with each other. 3 nodes were used during the implementation: a wrapper node for the LiDAR sensor, a wrapper node for the pan-tilt turret node, and an MAV detection and tracking node. The wrapper node for the LiDAR sensor node fixes some conversion issues of the incoming point cloud. The wrapper node for the pan-tilt turret node has the main role of converting the MAV position estimate from the main node to turret commands. The MAV detection and tracking node holds the main algorithm including the particle filter.

IV. INDOOR EXPERIMENTS AND EVALUATION

First, the results of the experiments are presented and analyzed beginning with the initial detection of the MAV after building the background model. Second, the main part of the algorithm, the tracking, is analyzed in terms of accuracy, as well as its capabilities concerning the loss of tracking.

The experiments were conducted within the MIMO arena [25] within the HUN-REN SZTAKI Institute for Computer Science and Control incorporating an OptiTrack motion capture system in a $7 \times 8 \text{ m}^2$ office space with a height of 3.5 m . Further hardware includes MAVs (Crazyflie 2.0 by Bitcraze), the turret (WidowX Dual XM430 Pan & Tilt turret by Trossen Robotics), and the rosette scanning LiDAR (Avia LiDAR sensor by Livox) with an integration time of 100 ms (10 Hz).

In all our experiments the particle filter was run at 15 Hz frequency which assured the processing of all LiDAR measurements.

A. Detecting the MAV

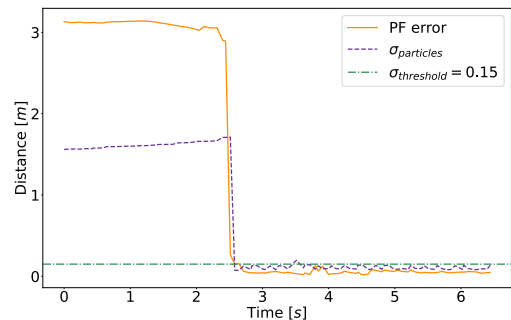


Fig. 2: Initial detection error and $\sigma_{particles}$ of the particle filter. The particle filter locks onto the drone almost instantaneously after receiving the first measurement at around 2.5 seconds.

Fig. 2 shows the error as the distance of the estimated state to the true state in meters of a representative detection. The average of the standard deviation of the particles in each dimension is also plotted (denoted as $\sigma_{particles}$).

When there is no incoming measurement only the predict step of the particle filter is performed. This adds a random zero mean noise with a set σ_{pred} to the particles which increases the overall $\sigma_{particles}$. In all of our experiments $\sigma_{pred} = 0.1 \text{ m}$, which turned out to be a good compromise between being able to track fast-moving drones and providing accurate measurements.

While the drone is out of the FoV of the LiDAR sensor, the particles remain idle, only influenced by the added noise in the predict step which results in a slowly inflating particle cloud with a slowly rising $\sigma_{particles}$. In this case, the MAV is resting on the floor and, because of its small size, is hidden inside the background model. As the drone starts hovering and measurements of it arrive at around 2.5 seconds the particles gather and allow for the first good estimation. Parallel with this the $\sigma_{particles}$ of the estimation drops sharply. The tracking can be considered stable when $\sigma_{particles}$ is around the parameter σ_{pred} . $\sigma_{particles}$ increases with about σ_{pred} in the first iterations, so the tracking is stable if it is under $\sigma_{threshold} = 1.5 \times \sigma_{pred}$ which is also shown in the figure.

B. Tracking the MAV

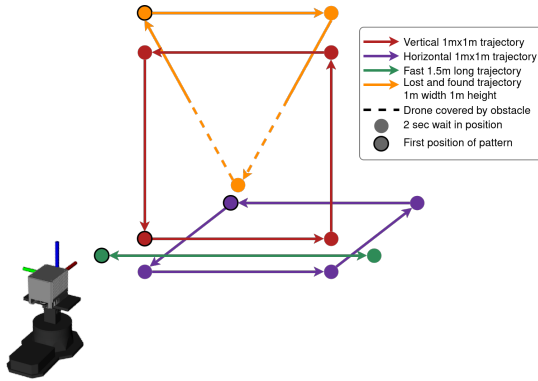


Fig. 3: Different drone testing flight patterns with different colors (vertical, horizontal, fast, and 'lost and found'). The outlined circles show the starting position of each trajectory while the arrows denote the moving direction of the drone. The dashed part of the arrow means that the MAV view is obstructed from the LiDAR's point of view by an obstacle. The size of each trajectory is in the legend of the figure.

For calculating the accuracy, the MAV was flown following certain flight patterns in Fig. 3 in a repeated manner. The ground truth data was obtained by the motion capture system within the MIMO arena by recording the pose of the LiVOX sensor and the position of the drone and aligning the LiVOX measurements with the MIMO arena using the recorded pose. The patterns in Fig. 3 were drawn from the point of view of the LiDAR sensor where the middle of each trajectory in the horizontal direction was in front of the sensor with a minimum distance of around 3 m. Each circle represents a stationary wait time of 2 s and the one with a black outline represents the first position of the respective pattern. The trajectory represented by the arrows in-between was flown in 3 s in case of the vertical, horizontal, and 'lost and found' pattern which resulted in a maximum speed of about 0.6 m/s, while it was flown in 2.25 s in case of the fast pattern which resulted in a maximum speed of around 1.2 m/s. In each experiment, the drone flies to the first point and then it flies the pattern 3 times in the case of the vertical and horizontal patterns and 4 times in the case of the others.

In Fig. 4, the error of the particle filter is plotted with the ground truth speed calculated from the MIMO measurements assuming constant speed between positions. It is visible that the tracking is stable over time with an average position error of around 5 cm in the case of the horizontal and vertical measurements while it is around 7.5 cm for the fast pattern. Each recording starts with the drone flying to the first position which can be seen on the first peak of each plot, where the speed and error characteristics are different than the later ones.

It can be seen on all the plots of Fig. 4, that the error of the particle filter is very much dependent on the speed. When the drone is at a waypoint, not moving, the error of the filter is around 4 to 5 cm, while at the peak speed of

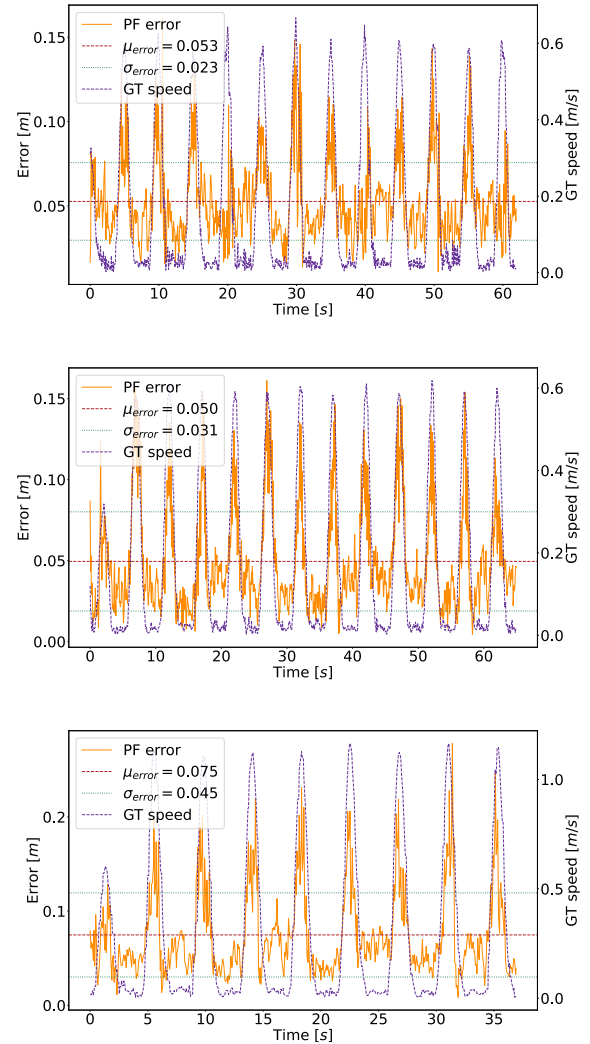


Fig. 4: Position error of the the particle filter plotted together with ground truth speed from the MIMO arena for the vertical (top), horizontal (middle), and fast (bottom) patterns. The mean (μ_{error}) and standard deviation ($\pm\sigma_{error}$) of the particle filter error is also plotted.

1.2 m/s of the fast pattern the error is around 20 to 25 cm. This dynamic difference of 15 to 20 cm in the error can mostly be explained by the different delays in the pipeline. The internal processing time of the LiDAR firmware is 2 ms based on the data-sheet, the LiDAR scan integration time is 100 ms, and there is some additional overhead in the formatting, stamping, and publishing of the data to ROS topics. The background subtraction and the application of filters took 6.1 ms with a $\sigma = 6.1$ ms standard deviation on the fast trajectory and the predict, update and resample steps took a combined 1.4 ms with a $\sigma = 0.2$ ms. The whole delay is about 120 ms, in which the drone travels about 14.4 cm.

The inner workings of the particle filter mean that the particles will always be a little behind the measurements.

Furthermore, the relative movement of the drone and the LiDAR sensor also causes some smearing in the point cloud which explains the rest of the dynamic error.

Overall the static tracking error is very small and constant. The dynamic error increases linearly with speed not impacting the robustness of tracking only the accuracy.

For comparison, in [26] the RMSE is reported as the metric of accuracy on different trajectories. From their paper, the trajectory T1 is most similar to our horizontal pattern and the trajectory T3 is most similar to our vertical case. We consider them similar because the trajectories are mostly in the horizontal and vertical planes respectively and mostly contain straight lines and turns close to right angles. Their reported best RMSE for T1 and T3 are 0.0773 m and 0.0421 m while the RMSE for our horizontal and vertical patterns are 0.0624 m and 0.0481 m respectively. While the two methods work very similarly in terms of accuracy, our particle filter approach has the added benefit of being able to regain tracking after it was lost and was extensively tested outside.

C. Losing and regaining Tracking

An advantage of utilizing a particle filter is that the detection and tracking properties are part of the same routine, which leads to good performance in terms of regaining tracking after the target is lost.

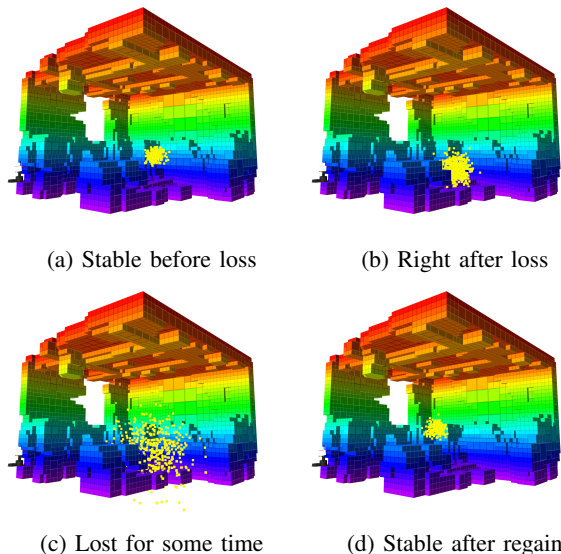


Fig. 5: Different stages of the particle cloud during tracking loss and regain. The particle cloud can be seen with yellow in front of the OctoMap of the background model. The number of particles was 500 in this experiment.

Fig. 5 shows a typical loss and regain event of the MAV tracking from (a) to (d) while Fig. 6 shows the corresponding error and $\sigma_{particles}$ characteristics. This is one traversal of the drone through the 3 waypoints of the 'lost and found' pattern. First, the normal MAV tracking is depicted in Fig 5a. The particles are grouped around the drone with $\sigma_{particles} < 0.15\text{ m}$. When the drone starts moving, the error increases

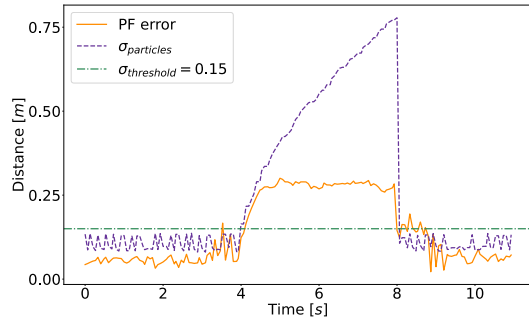


Fig. 6: Particle filter error and $\sigma_{particles}$ are plotted together for a typical loss and regain event. The tracking was lost at around 4 seconds and was regained at 8 seconds.

slightly but the tracking is still stable. At around 4 seconds the drone gets behind the obstacle and $\sigma_{particles}$ increases over 0.15 m meaning the tracking is lost and the particle cloud starts inflating (Fig. 5b). The particle cloud inflates further to almost $\sigma_{particles} = 0.8\text{ m}$ which is depicted on Fig. 5c while the error stays constant because the drone hovers behind the obstacle and the estimated pose is the mean of the particle positions which is at the position where the tracking was lost. Then the drone flies out from behind the cover and the particle update and resample steps of the filter condense the cloud instantly which is well depicted on the sharp drop of $\sigma_{particles}$ below 0.15 m in Fig. 6. The tracking is stable again in Fig. 5d and the error also decreases to the static error at about 9 seconds when the drone stops moving.

Overall the regaining of tracking after loss is practically instantaneous allowing robust tracking even in scenarios where the trajectory is partially occluded.

V. OUTDOOR FIELD TESTS AND COMPARISON

After the successful indoor tests, we validated the developed method in an outdoor environment as well. We performed the measurements with the presented method under two different weather conditions (on a sunny and a foggy day). The purpose of the validation is to test the track movement and to determine the detection distances and number of detected points in outdoor conditions, on a commercial drone. Finally, we compared the performance of our method to the previous state-of-the-art [13].

A. Outdoor test

For outdoor tests, the DJI Phantom drone was used on approximately flat terrain. DJI Phantom 4 Pro V2.0 measures $251\text{ mm} \times 398.78\text{ mm} \times 172.72\text{ mm}$ and weighs 1375 g with a battery and propellers attached. An important parameter for detection is the frame size (the largest distance between the motors), which is 350 mm for this type of drone. The measurements were carried out in the factory state of the drone, we did not improve the detection range by using special paint or other methods. For a video of the

outdoor experiment, kindly check the video attachment here: <https://youtu.be/VdePm3on8vo>.



Fig. 7: Weather on the test days. Sunny experiment with clouds on the left and the foggy experiment with severely limited viewing conditions on the right.

A sunny day was chosen for the first and a foggy day for the second measurement day when visibility was also severely limited (see Fig.7).

B. Results

During both tests, the drone was moving under such conditions that both horizontal and vertical distances could be analyzed. In both cases, the controlled pan-tilt turret followed the drone correctly, thus the drone tracking was successful.

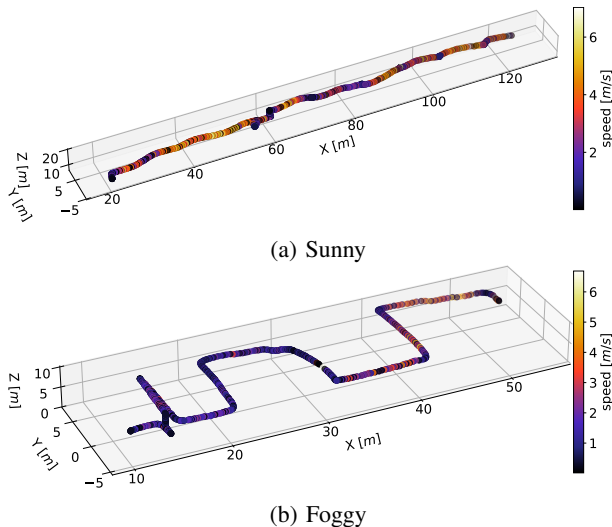


Fig. 8: Trajectory and speed of the drone on a sunny and foggy day. The turret was at the origin of the coordinate system.

When evaluating drone detection, an important value is the maximum detection distance. The drone’s trajectory was successfully tracked up to a distance of 128 m in the sunny test environment (Fig. 8a), and up to a distance of 58 m in the foggy test environment (Fig. 8b). As explained earlier in subsection IV-A, we consider the drone tracked when $\sigma_{particles} < 0.15$ m. We consider the tracking lost after 10 subsequent missing measurements, but it is important to note that we had some occasional detections at distances of up to 145 m on the sunny day.

In both scenarios, we calculated maximum speeds of a little more than 6 m/s from the tracking positions and timestamps.

C. Comparison

We compare our outdoor test results with another study in which the drone detection efficiency of the VLP-16 LiDAR was tested. In the work of Dogru et al.[13], the size of the drones is larger than the one used for our measurement, which affects the number of reflected points. Furthermore in their paper, there are measurements in which a retroreflector was used to increase the number of points reflected to the sensor.

TABLE I: Comparison of maximum detection distances

Measurement, method	Weather	With retroreflector	Distance(m)
Our test I.	Sunny	No	128
Our test II.	Foggy	No	58
Dogru et al.[13]	Sunny	Yes	100
Dogru et al.[13]	Sunny	No	70

Our maximum distance of detection is about 1.5 to 2 times greater than their result as in TABLE I.

Another important aspect is the number of detected points, which greatly impacts the robustness of tracking. In sunny weather, except for the last part of the detection range, the number of detected points in the result is 3 to 5 times higher than in the current state-of-the-art (see Fig. 9).

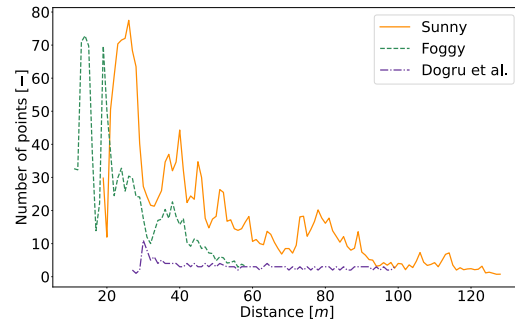


Fig. 9: Number of detected points depending on distance. The proposed algorithm returns significantly more points in every distance range than [13].

In the case of foggy weather, the detection distance was significantly reduced, as expected in advance based on the literature[40].

VI. CONCLUSION

This article presents a novel tracking method using a rosette scanning LiDAR, which controls a Pan-Tilt turret based on the estimated position of the detected drone in order to keep the object in the center of the FoV. The static background model created in the initializing phase of the algorithm is extracted from the point cloud during tracking. The drone’s position is calculated using a particle filter after processing and filtering the incoming point cloud.

The proposed algorithm was tested in indoor and outdoor environments as well. Based on the test results, our proposed method has the accuracy of the current state-of-the-art indoor method[26], while significantly outperforming the state-of-the-art outdoor method[13] in terms of detection range and returned number of points. To conclude, our proposed method is a valid solution for drone detection and tracking using LiDAR sensor.

REFERENCES

- [1] S. Mohsan, N. Othman, Y. Li, M. Alsharif, and M. Khan, "Unmanned aerial vehicles (uavs): practical aspects, applications, open challenges, security issues, and future trends," *Intelligent Service Robotics*, 2023.
- [2] A. Rejeb, A. Abdollahi, K. Rejeb, and H. Treiblmaier, "Drones in agriculture: A review and bibliometric analysis," *Computers and Electronics in Agriculture*, 2022.
- [3] O. Maghazei and T. Netland, "Drones in manufacturing: Exploring opportunities for research and practice," *Journal of Manufacturing Technology Management*, vol. Forthcoming, 2019.
- [4] N. T. K. Chi, L. T. Phong, and N. T. Hanh, "The drone delivery services: An innovative application in an emerging economy," *The Asian Journal of Shipping and Logistics*, 2023.
- [5] J. Shahmoradi, E. Talebi, P. Roghanchi, and M. Hassanalian, "A comprehensive review of applications of drone technology in the mining industry," *Drones*, 2020.
- [6] A. Petrovski and M. Radovanović, "Application of drones with artificial intelligence for military purposes," 10 2022.
- [7] R. L. Wilson, "Ethical issues with use of drone aircraft," in *2014 IEEE International Symposium on Ethics in Science, Technology and Engineering*, 2014.
- [8] A. Vacca and H. Onishi, "Drones: military weapons, surveillance or mapping tools for environmental monitoring? the need for legal framework is required," *Transportation Research Procedia*, 2017.
- [9] J. Łukasiewicz and A. Kobaszyńska Twardowska, "Proposed method for building an anti-drone system for the protection of facilities important for state security," *Security and Defence Quarterly*, 2022.
- [10] A. Coluccia, G. Parisi, and A. Fascista, "Detection and classification of multirotor drones in radar sensor networks: A review," *Sensors*, 2020.
- [11] J. Zhao, X. Fu, Z. Yang, and F. Xu, "Radar-assisted uav detection and identification based on 5g in the internet of things," *Wireless Communications and Mobile Computing*, 2019.
- [12] M. Hammer, M. Hebel, M. Arens, and M. Laurenzis, "Lidar-based detection and tracking of small uavs," 2018.
- [13] S. Dogru and L. Marques, "Drone detection using sparse lidar measurements," *IEEE Robotics and Automation Letters*, 2022.
- [14] M. Vrba and M. Saska, "Marker-less micro aerial vehicle detection and localization using convolutional neural networks," *IEEE Robotics and Automation Letters*, 2020.
- [15] V. Walter, N. Staub, A. Franchi, and M. Saska, "Uvdar system for visual relative localization with application to leader-follower formations of multirotor uavs," *IEEE Robotics and Automation Letters*, 2019.
- [16] A. Carrio, S. Vemprala, A. Ripoll, S. Saripalli, and P. Campoy, "Drone detection using depth maps," in *2018 IEEE/RSJ International Conference on Intelligent Robots and Systems (IROS)*, 2018.
- [17] I. Nemer, T. Sheltami, I. Ahmad, A. Yasar, and M. Abdeen, "Rf-based uav detection and identification using hierarchical learning approach," *Sensors*, 2021.
- [18] O. O. Medaiyese, M. Ezuma, A. P. Lauf, and I. Guvenc, "Wavelet transform analytics for rf-based uav detection and identification system using machine learning," *Pervasive and Mobile Computing*, 2022.
- [19] G. Corzo, E. Alvarez-Aros, J. Mariño, and N. Amézquita-Gómez, "Military artificial intelligence applied to sustainable development projects: sound environmental scenarios," *DYNA*, 09 2023.
- [20] S. Al-Emadi, A. Al-Ali, and A. Al-Ali, "Audio-based drone detection and identification using deep learning techniques with dataset enhancement through generative adversarial networks," *Sensors*, 2021.
- [21] F. Svanstrom, C. Englund, and F. Alonso-Fernandez, "Real-time drone detection and tracking with visible, thermal and acoustic sensors," 2020.
- [22] J. Dudczyk, R. Czyba, and K. Skrzypczyk, "Multi-sensory data fusion in terms of uav detection in 3d space," *Sensors*, 2022.
- [23] F. Svanström, F. Alonso-Fernandez, and C. Englund, "Drone detection and tracking in real-time by fusion of different sensing modalities," 2022.
- [24] D. Rozenberszki and A. Majdik, "The mta sztaki micro aerial vehicle and motion capture arena," *MTA SZTAKI*, 2019.
- [25] S. Gazdag, A. Kiskaroly, T. Sziranyi, and A. L. Majdik, "Autonomous racing of micro air vehicles and their visual tracking within the micro aerial vehicle and motion capture (mimo) arena," in *ISR Europe 2022; 54th International Symposium on Robotics*, 2022.
- [26] I. Catalano, H. Sier, X. Yu, T. Westerlund, and J. P. Queralta, "Uav tracking with solid-state lidars: Dynamic multi-frequency scan integration," in *2023 21st International Conference on Advanced Robotics (ICAR)*, 2023, pp. 417–424.
- [27] J. Redmon, S. Divvala, R. Girshick, and A. Farhadi, "You only look once: Unified, real-time object detection," in *2016 IEEE Conference on Computer Vision and Pattern Recognition (CVPR)*, 2016.
- [28] L. Spinello, K. Arras, R. Triebel, and R. Siegwart, "A layered approach to people detection in 3d range data," *Proceedings of the AAAI Conference on Artificial Intelligence*, 2010.
- [29] D. Maturana and S. Scherer, "3d convolutional neural networks for landing zone detection from lidar," *Proceedings - IEEE International Conference on Robotics and Automation*, 2015.
- [30] Y. Zhou and O. Tuzel, "Voxelnet: End-to-end learning for point cloud based 3d object detection," in *2018 IEEE/CVF Conference on Computer Vision and Pattern Recognition*, 2018.
- [31] C. R. Qi, H. Su, K. Mo, and L. J. Guibas, "Pointnet: Deep learning on point sets for 3d classification and segmentation," 2016.
- [32] C. R. Qi, L. Yi, H. Su, and L. J. Guibas, "Pointnet++: Deep hierarchical feature learning on point sets in a metric space," 2017.
- [33] A. Dewan, T. Caselitz, G. D. Tipaldi, and W. Burgard, "Motion-based detection and tracking in 3d lidar scans," in *IEEE International Conference on Robotics and Automation (ICRA)*, 2016.
- [34] F. Moosmann and C. Stiller, "Joint self-localization and tracking of generic objects in 3d range data," in *Proceedings of the IEEE International Conference on Robotics and Automation*, Karlsruhe, Germany, 2013.
- [35] J. Razlaw, J. Quenzel, and S. Behnke, "Detection and tracking of small objects in sparse 3d laser range data," 2019.
- [36] C. Romero-González, Álvaro Villena, D. González-Medina, J. Martínez-Gómez, L. Rodríguez-Ruiz, and I. García-Varea, "Inlida: A 3d lidar dataset for people detection and tracking in indoor environments," in *Proceedings of the 12th International Joint Conference on Computer Vision, Imaging and Computer Graphics Theory and Applications - Volume 6: VISAPP, (VISIGRAPP 2017)*, 2017.
- [37] L. Qingqing, Y. Xianjia, J. P. Queralta, and T. Westerlund, "Adaptive lidar scan frame integration: Tracking known mavs in 3d point clouds," 2021.
- [38] R. Rasshofer, M. Spies, and H. Spies, "Influences of weather phenomena on automotive laser radar systems," *Advances in Radio Science*, 2011.
- [39] R. Heinzler, P. Schindler, J. Seekircher, W. Ritter, and W. Stork, "Weather influence and classification with automotive lidar sensors," in *2019 IEEE Intelligent Vehicles Symposium (IV)*, 2019.
- [40] M. Bijelic, T. Gruber, and W. Ritter, "A benchmark for lidar sensors in fog: Is detection breaking down?" in *2018 IEEE Intelligent Vehicles Symposium (IV)*, 2018.
- [41] A. Filgueira, H. González-Jorge, S. Lagüela, L. Díaz-Vilariño, and P. Arias, "Quantifying the influence of rain in LiDAR performance," *Measurements*, 2017.
- [42] N. J. Gordon, D. J. Salmond, and A. F. Smith, "Novel approach to nonlinear/non-gaussian bayesian state estimation," in *IEE proceedings F (radar and signal processing)*, 1993.
- [43] A. Hornung, K. M. Wurm, M. Bennewitz, C. Stachniss, and W. Burgard, "OctoMap: An efficient probabilistic 3D mapping framework based on octrees," *Autonomous Robots*, 2013.
- [44] R. B. Rusu and S. Cousins, "3D is here: Point Cloud Library (PCL)," in *IEEE International Conference on Robotics and Automation (ICRA)*, 2011.
- [45] J. Elfring, E. Torta, and R. van de Molengraft, "Particle filters: A hands-on tutorial," *Sensors*, 2021.